Active contours for multi-region image segmentation with a single level set function

Anastasia Dubrovina and Ron Kimmel

August 15, 2012

Abstract

Segmenting an image into similar parts is important for low level image understanding. Many formulations of the segmentation task have been suggested over the years. While axiomatic functionals, such as the Mumford-Shah functional, are hard to implement and analyze, graph-based alternatives often impose artificial measures on the problem. The latter are usually simple to optimize and implement at the expense of giving up some desired properties.

Here, we tackle the most basic image quantization, or piecewise constant segmentation problem, while regularizing the boundaries between the regions according to a weighted Euclidean arc-length. The problem is shown to be related to the original Mumford-Shah functional, and formalized as a level set evolution equation. Yet, unlike most existing methods, the evolution is executed using a single non-negative level set function, through the Voronoi Implicit Interface Method [21] for a multi-phase interface evolution. The proposed framework has been tested on a number of synthetic and real images, with different number of regions, and compared to a state-of-the-art algorithm for image segmentation.

1 Introduction

Image segmentation is important for object detection and classification, scene understanding, action classification, and other visual information analysis tasks. In this paper we consider active contour approaches, which have been proven to be extremely successful for that goal. They can be roughly divided into edge-based methods [11, 5, 12, 6], region-based techniques [14, 8, 10, 13, 9, 3], and combined approaches [27, 16, 19], to mention just a few.

Generally, the active contour evolution is performed using the level set framework [15], which helps overcome inherited implementation difficulties associated with spline-based approaches. The level set framework, when utilized per se, is geared towards two-region image segmentation. To alleviate this limitation, various methods were developed; all of them, however, require managing *multiple* level set functions. Some associate a level set function with each image region, and evolve these functions in a coupled manner [26, 25, 20]. Others perform hierarchical segmentation, by iteratively splitting previously obtained regions using the conventional level set framework [23, 4]. These methods too require coupled level set evolution, so that the resulting regions do not develop gaps or overlaps. It is also possible to use a smaller number of level set functions, say n, and segment an image into 2^n regions [24].

A different approach to image segmentation consists of formulating it as a discrete labeling problem, and solving it using graph-cuts or convex relaxation algorithms [18, 17, 7]. These methods were developed for a certain type of problems [7], but currently are not suited for different energy measures, for instance, the *elastica* term in [11] (integral of the squared curvature of the evolving contour). In addition, they usually require knowing the number of regions a priori.

In contrast to the methods described above, the approach suggested in this paper allows segmenting images with unknown number of possibly overlapping objects, according to some desired energy measure. For this purpose we utilize a novel level set framework for multi-phase, or multi-region interface evolution, named the Voronoi Implicit Interface Method (VIIM), which was introduced by Saye and Sethian in [21]. According to it, the evolution is performed using a *single* non-negative level set function, while implicitly dealing with region merging and splitting.

Our main contributions can be summarized as follows: first, we review the axiomatic formulation of the multi-region image segmentation problem as an energy functional minimization. Specifically, we consider the approximately piecewise constant image model. We derive the active contour evolution equation minimizing the above energy functional, formulate it as the level set evolution problem, and solve it by utilizing the VIIM level set framework. The proposed method does not require knowing the number of the regions in the image or their statistics a priori, and produces good segmentation results for various initial contours. We compare the output of the proposed method with the two-region piecewise constant model of Chan and Vese [8] and the convex relaxation method of Chambolle and Pock [7].

The structure of the paper is as follows: in the next section we review the

Voronoi Implicit Interface Method. In Section 3 we formulate the multiple regions segmentation problem, and derive its active contour evolution equation. In Section 4 we extract the corresponding level set evolution equation in terms of the VIIM framework, and formalize the suggested segmentation method. In Section 5 we present segmentation results obtained with the proposed method for different types of images, and compare them to results obtained using [7]. Section 6 concludes the paper and describes potential extensions of the proposed framework.

2 Review of the Voronoi Implicit Interface Method

The VIIM was developed in order to solve interface propagation problems with arbitrary number of phases, or regions, in m-dimensional Euclidean space. In 2D the interface separating between different phases is a curve, possibly with multiple junctions. In 3D, the interface consists of two-dimensional surfaces. Illustrations of 2D and 3D interfaces can be found in [21].

The interface propagation is performed using a *single* non-negative level set function $\phi(\mathbf{x}), \mathbf{x} \in \mathbb{R}^m$, given by the unsigned distance from the interface Γ, and defined on a fixed regular Eulerian background mesh. The propagation is governed by the following PDE

$$\phi_t = F_{ext} \left|\nabla \phi\right|, \tag{1}$$

where F_{ext} is the extension of the interface propagation speed F to the whole m-dimensional region. The examples in [21] include curvature and mean curvature flows, as well as physical simulations of the dynamics of dry foams.

The central idea of the VIIM is as follows: assume we are given a zero level set of a function ϕ, and a velocity F defined along it. We can extend this velocity to the neighboring level sets in a smooth manner, to obtain the extension velocity F_{ext} and apply Eq. (1). Then, two evolving ϵ-level sets will always encapsulate the evolving zero level set they are adjacent to. Moreover, the ϵ-level sets of ϕ are simple curves, without multiple-junction points, and their evolution is well defined. Thus, the evolved ϵ-level sets of the level set function can be used to reconstruct the evolving interface, which is assumed to lie at an equal distance from the two ϵ-level sets adjacent to it. It is calculated using the Voronoi regions of the ϵ-level sets.

In order to evolve the interface as described above, Saye and Sethian suggested the following three step-algorithm (in $\mathbb{R}^2$).

1. First, advance the level set function ϕ by solving Eq. (1), with an appropriate time step.
2. Find the ϵ-level sets of the new function. Reconstruct the interface Γ to be the intersections of the Voronoi regions of the ϵ-level sets, calculated in the regions $\{(x,y) : \phi(x,y) < \epsilon\}$. Use the reconstructed interface Γ to update the unsigned distance function ϕ.
3. Update the propagation speed function F, and return to 1.

The VIIM is formulated in terms of a general interface velocity F, and thus it is applicable for various interface evolution problems utilizing the level set approach. Below, we show how it can be employed for multiple regions image segmentation, where the active contour acts as an interface, and the regions it defines are the phases in the VIIM notation.

3 Multiple regions image segmentation

A general energy functional describing an active contour model may be written as

$$E(C) = E_{image}(C) + \mu E_{contour}(C). \tag{2}$$

The data term $E_{image}(C)$ measures the quality of the segmentation provided by the contour C. It may originate from various image models, such as the piecewise-smooth or piecewise-constant models of [14, 8], statistical models of [10, 13], etc. The regularization term $E_{contour}(C)$ may depend on the contour properties alone [11, 14], or incorporate image information as well [5, 6].

In this paper we consider a special case of the regularized piecewise-constant model for multi-region image segmentation, which is closely related to the piecewise-smooth model of [14]. We start with a review of the two-region model based on [8, 6]. We then extend it for multiple regions, and derive the corresponding active contour evolution equations.

3.1 Piecewise constant model with GAC regularization

We use the formulation according to which the energy is given by

$$\begin{aligned} E(C, c_1, c_2) &= \iint_{\Omega_C} (I(x,y) - c_1)^2 \, dxdy + \iint_{\Omega \setminus \Omega_C} (I(x,y) - c_2)^2 \, dxdy \\ &\quad + \mu \oint_C g(C(s))ds, \end{aligned} \tag{3}$$

where $I(x, y)$ denotes the image, defined on a 2D domain Ω, C is the interface contour, and Ω_C and $\Omega \backslash \Omega_C$ are the regions inside and outside the contour C, respectively. When optimized for, c_1 and c_2 are the mean grayscale values of the image I in Ω_C and $\Omega \backslash \Omega_C$. The last term of $E(C, c_1, c_2)$ is an interface regularization term, measuring a weighted contour length. The function g is an edge indicator function [6], e.g. $g(x, y) = \frac{1}{1+|\nabla \hat{I}|}$, where $\hat{I}$ is a smoothed version of I, or $g(x, y)$ suggested in [19] for color images. The parameter μ controls the weight of the regularization term in the total energy.

The active contour evolution rule is given by the first variation of the functional with respect to the evolving curve C,

$$C_t = -\frac{\delta E}{\delta C} = -\left((I - c_1)^2 - (I - c_2)^2\right) \mathbf{n} + \mu \left(\kappa g - \langle \nabla g, \mathbf{n} \rangle\right) \mathbf{n}, \quad (4)$$

where $\mathbf{n}$ is the normal to the curve C. The level set formulation of (4) is

$$\phi_t = -\left((I - c_1)^2 - (I - c_2)^2\right) |\nabla \phi| + \mu \mathrm{div} \left(g(x, y) \frac{\nabla \phi}{|\nabla \phi|} \right) |\nabla \phi|. \quad (5)$$

The values c_1 and c_2 minimizing the energy $E(C, c_1, c_2)$ are given by

$$c_1 = \frac{\iint_{\Omega_C} I(x, y)^2 dxdy}{\iint_{\Omega_C} dxdy} \quad , \quad c_2 = \frac{\iint_{\Omega \backslash \Omega_C} I(x, y)^2 dxdy}{\iint_{\Omega \backslash \Omega_C} dxdy}. \quad (6)$$

3.2 Back to Mumford-Shah: Multiple regions segmentation model

Following the energy formulation for two regions, given in Eq. (3), we extend it to multiple regions segmentation as follows

$$E_{MR}(C, \{c_i\}) = \sum_i \iint_{\Omega_i} (I(x, y) - c_i)^2 \, dxdy + \mu \oint_C g(C(s)) ds. \quad (7)$$

The contour C now separates multiple regions, denoted by Ω_i, and may have multiple-junction points. Note that this is a modified version of the Mumford-Shah energy functional [14], in the sense that the regularization term is given by the Geodesic Active Contours.

In order to simplify the notations, we denote the different terms of the total energy (7) as follows

$$\begin{aligned} E^i_{CV}(C) &= \iint_{\Omega_i} (I(x, y) - c_i)^2 \, dxdy, \\ E_{GAC} &= \oint_C g(C(s)) ds. \end{aligned} \quad (8)$$

Thus, the energy can be written as

$$E_{MR}(C,\{c_i\}) = \sum_i E^i_{CV}(C) + \mu\, E_{GAC}. \tag{9}$$

Its first variation with respect to C is

$$\frac{\delta E_{MR}}{\delta C} = \sum_i \frac{\delta E^i_{CV}}{\delta C} + \mu\, \frac{\delta E_{GAC}}{\delta C}. \tag{10}$$

In order to find expressions for the first variations of the energy terms $E^i_{CV}(C)$, we will use the following Lemma [27].

Lemma 1. *The first variation of a functional*

$$E_W(C) = \iint_{\Omega_C} f(x,y)dxdy \tag{11}$$

is given by

$$\frac{\delta E_W(C)}{\delta C} = -f(x,y)\mathbf{n}. \tag{12}$$

We thereby obtain

$$\frac{\delta E^i_{CV}(C(x,y))}{\delta C} = -\left(I(x,y) - c_i\right)^2 \mathbf{n}, \quad (x,y) \in C_i, \tag{13}$$

where C_i denotes the part of the contour C that bounds the region Ω_i. We also denote by C_{ij} the contour segment shared by two regions Ω_i and Ω_j.

The second term of the total energy E_{MR}, E_{GAC}, is the familiar geodesic active contour energy term; its first variation is given in Eq. (4). Thus, the first variation of the multi-phase energy functional E_{MR} with respect to the evolving contour C is given by

$$\begin{aligned} \frac{\delta E_{MR}(C(x,y))}{\delta C} \quad &= \quad -\sum_{i,j} \Big((I(x,y) - c_i)^2 - (I(x,y) - c_j)^2 \Big) \, \mathbf{n} \\ &\quad + \mu \left(\kappa g - \langle \nabla g, \mathbf{n} \rangle \right) \mathbf{n}, \qquad (x,y) \in C_{ij}. \end{aligned} \tag{14}$$

Note that this result coincides with the result obtained by Mumford and Shah for a piecewise smooth segmentation model instead of a piecewise constant one using a different analysis and assuming $g = 1$ (see Sec. 2 of [14]).

Finally, the values $\{c_i\}$ minimizing the energy functional $E_{MR}(C,\{c_i\})$ are given by

$$c_i = \frac{\iint_{\Omega_i} I(x,y)^2 dxdy}{\iint_{\Omega_i} dxdy}. \tag{15}$$

4 Multiple-region segmentation using the VIIM

In this section we describe how to perform evolution of a boundary contour according to Eq. (14), using the VIIM framework. The contour, or interface velocity $F(C)$, is well defined, except for the junction points, and is given by

$$F(C(x,y)) = -\left((I-c_i)^2 - (I-c_j)^2\right) + \mu \mathrm{div}\left(g(x,y)\frac{\nabla\phi}{|\nabla\phi|}\right), \qquad (16)$$

for (x, y) laying along the contour segment C_{ij}. In order to use the VIIM formulation, we need to define the extension velocity F_{ext} for the ϵ-level sets evolution. We observe that a straight forward definition $F_{ext}(x, y) = F(x, y)$, $(x, y) \in \Omega_i$ using (16) will produce a velocity profile with discontinuities at the boundaries of the Voronoi regions of different contour segments. This is also related to the fact that the interface velocity F is not well defined at the junction points.

Instead, following the original philosophy of the VIIM, we would like to evolve the level set function in each region based on the information coming from this region alone. Therefore, we suggest using an extension velocity defined such that in a certain region it is based only on the local information of that region, as follows

$$F_{ext}(x,y) = -\left(I(x,y)-c_i\right)^2 + \mu \mathrm{div}\left(g(x,y)\frac{\nabla\phi}{|\nabla\phi|}\right), \qquad (x,y)\in\Omega_i. \qquad (17)$$

Proposition 1. *Assume that the level set function is given by an unsigned distance function from the evolving contour. For $\epsilon \ll 1$, the extension velocity $F_{ext}(x, y)$ defined in Eq. (17) will move every regular point (x, y) on the contour in the direction of the velocity $F(C(x, y))$ defined by the Euler-Lagrange equation (16).*

According to the proposition above, the contour evolution under the velocity F_{ext} (17), will be along the same direction as it would have been under the original velocity $F(C(x, y))$. Proof of Prop. 1 is given in Appendix A. Experimentally we found that the suggested extension velocity produces valid segmentation results, that, in case of the two-region problem, are similar to the results of the original formulation in Eq. (5).

The proposed approach can be summarized as follows. Assume we are given an initial contour C and the corresponding unsigned distance level set function $\phi(x, y)$.

1. Extend the interface velocity for each region using Eq. (17). Advance the level set function by solving the evolution equation (1).

2. Find the ϵ-level sets of the evolved level set function and reconstruct the interface using the Voronoi regions of the ϵ-level sets, as suggested by [21]. Calculate the new unsigned distance level set function ϕ.

3. Stop the evolution if a stopping criterion is met; otherwise, return to Step 1.

Implementation considerations: We used the forward Eulerian scheme to solve the evolution equation (1), and the fast marching method [22] to calculate the distance function ϕ and the Voronoi regions, at every iteration. To speed up the solution one can use operator splitting schemes for solving Eq. (1), with the narrow band approach of [1]. In order to prevent over-segmentation, we united separate regions with similar mean intensity values, as a part of Step 2 of the algorithm. In our implementation we used a threshold, denoted hereafter by T, set to 10% of the maximal image intensity value. For color images, we used the maximal absolute intensity difference among the three color channels.

We normalized the images to have intensity values in the range of $[0, 1]$. The algorithms parameters were set to the following values: $[0.02, 0.1]$ for the weight μ (Eq. (7)); $[25, 50]$ for the time step dt; $\epsilon = 0.1$ for the VIIM method. Mean absolute intensity difference threshold T for region merging was chosen as stated above. In order to approximate the level set function derivatives next to its zero-level set (where ϕ is not differentiable) we used forward- or backward-differences calculated using values of ϕ in each region separately. Note, that the width of the ϵ-level sets influences the size of the smallest features that the algorithm is able to segment. To capture small features one may up-sample the image before the segmentation, similar to the technique used in [2].

5 Experimental results

In this section we present segmentation results obtained with the proposed method for different types of images, and with different parameter choices.

Comparison to two-region model: In the first experiment we compared the proposed method with the two-region Chan-Vese formulation (3), both applied to an image consisting of two regions. The segmentation results are shown in Fig. 1, together with the initial contour. As expected, both algorithms produce similar results.

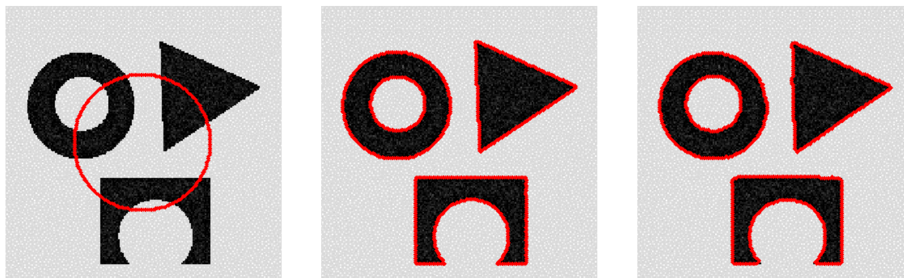

(a) (b) (c)

Figure 1: Comparison of the proposed method with the original two-region Chan-Vese. (a) Image with the initial contour, shown in red. (b) Segmentation obtained with two-region Chan-Vese formulation. (c) Segmentation obtained with the proposed method. The obtained contours defining object boundaries are shown in red.

Synthetic images with multiple regions: In our next experiment, we tested the algorithm on two synthetic images with several overlapping regions, boundaries of which meet at a number of triple-junctions. The first example, shown in Fig. 2, top, is of a grayscale image with added Gaussian noise with standard deviation equal to 5% of the image intensity range. The second example, shown in Fig. 2, bottom, is of a colored image, with added Gaussian noise with standard deviation equal to 10% of the image intensity range. In both examples, using the proposed method we were able to segment the images, despite the added noise. The parameters used for both images were: $\mu = 0.02$, $dt = 50$, $T = 10\%$ of the intensity range.

Comparison to a convex relaxation method for image segmentation: The proposed method was compared with the convex relaxation method of Chambolle and Pock [7]; segmentation results produced by both methods are presented in Fig. 3. To evaluate the latter method, we used a code published by the authors of [7], with the following parameters: isotropic TV, simple relaxation and mean values produced by k-means clustering, $K = 8$ (number of labels) and $\lambda = 5.0$ (the L_1-term weight, see [7]). From examining the images in Fig. 3, (d) and (e), we see that both methods produce similar results. Regions obtained with [7] have smoother boundaries, as it uses the contour length regularizer, while the proposed method, using geodesic active contours, tends to produce curved boundaries following high image gradients.

Additional segmentation results: Fig. 4 presents segmentation results obtained with the proposed method with different values of the threshold T.

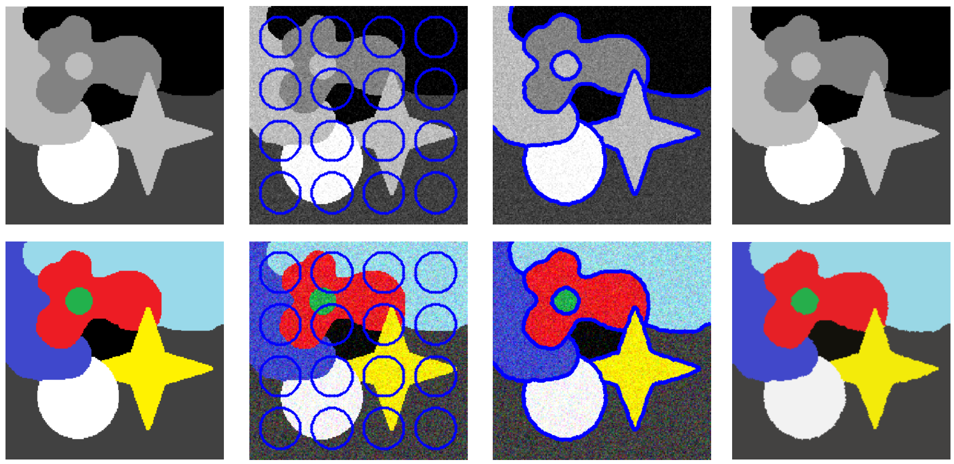

(a) (b) (c) (d)

Figure 2: Segmentation of noisy synthetic grayscale and color images with overlapping objects. (a) The original images. (b) Images with added noise and initial contour. (c) Segmentation results obtained with the proposed method. (d) Regions colored according to their mean intensity values.

Specifically, increasing T results in more regions being deemed similar and merged during the evolution process, thus producing less detailed segmentation. The results shown in Fig. 4 were compared to segmentation obtained with [7] applied to the same data. It was used with isotropic TV, simple relaxation, mean values obtained using k-means clustering, and varying values of K and λ, in order to obtain similar number of regions as with the proposed method. The results are shown in Fig. 5. We observe that in this case the convex relaxation approach produced inferior results, probably due to high non-homogeneity of the input image. Changing the parameters of the algorithm [7] did not produce significantly better results.

Example from the Berkeley Segmentation Dataset: The final test we performed was using an image from the Berkeley Segmentation Dataset[1]. Fig. 6 presents the segmentation results obtained with our method, with the convex relaxation of [7], and the ground-truth segmentation from the dataset. Both methods produce similar segmentation results, though the proposed algorithm fails to detect small image features, such as thin lines and tiny structures. This can be overcome by up-sampling the image prior to the segmentation. The algorithm of [7] on the other hand produces over-

[1] `http://www.eecs.berkeley.edu/Research/Projects/CS/vision/bsds/`

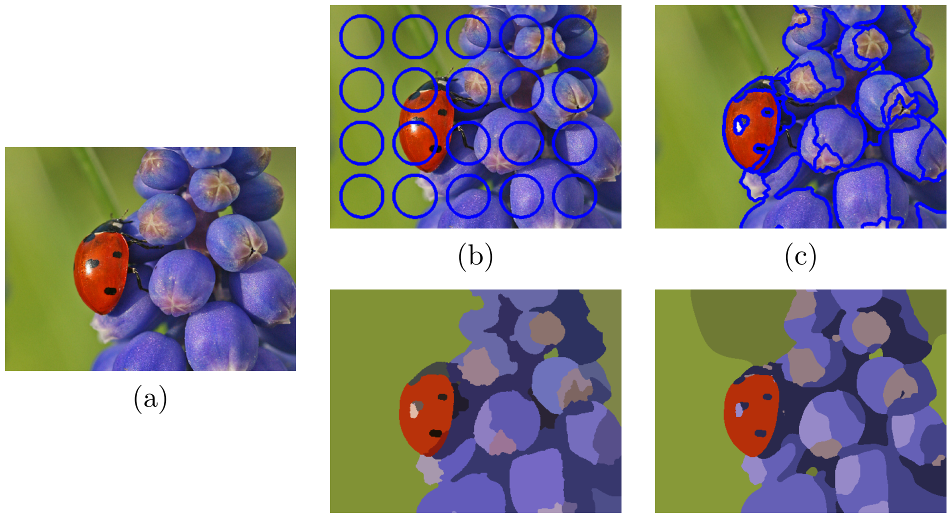

(a) (b) (c) (d) (e)

Figure 3: Comparison of the proposed method with convex relaxation approach of [7]. (a) The original image. (b) Initial contour used by our method. (c) Region boundaries detected by our method. (d) Regions detected by our method, colored according to their mean intensity values. (e) Segmentation result of [7].

segmentation, dividing the sky in the image into two parts. Using smaller K, equal to 6 for instance, does not resolve this problem.

6 Conclusions and future work

We addressed the problem of multi-region image segmentation, implementing a modified Mumford-Shah model where the geodesic active contour is used for boundary regularization. For implementation we used the Voronoi Implicit Interface Method which is a multi-phase level set formulation where the boundary contour is an ϵ-set rather than the traditional intersection set. This new formulation allowed us to deal with multiple segments simultaneously, while employing geometric constraints for the smoothness of boundaries between the image segments, all within the same framework. Extending the numerical support about the boundaries allowed us to overcome implementation difficulties of traditional geometric-variational segmentation methods. In this paper we limited our discussion to piecewise constant intensity profiles, a limitation that we plan to overcome in future research.

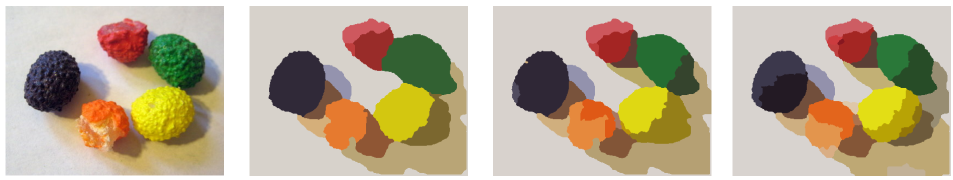

(a) (b) (c) (d)

Figure 4: Segmentation results obtained with the proposed method using different values of the absolute intensity difference T. (a) The original image. (b) $T = 20\%$. (c) $T = 15\%$. (d) $T = 10\%$.

(a) (a) (b) (c)

Figure 5: Segmentation results obtained with the convex optimization method of [7], with different algorithm parameters. (a) The original image. (b) $K = 8, \lambda = 5.0$. (c) $K = 12, \lambda = 6.0$. (d) $K = 16, \lambda = 8.0$.

Acknowledgements

The authors thank J.A. Sethian of UC Berkeley for intriguing discussions and introducing the VIIM to our group. This research was supported by European Community's FP7-ERC program, grant agreement no. 267414.

A Proof of Proposition 1

Assume that $(x, y) \in C$ is a point on the contour segment C_{ij} between the regions Ω_i and Ω_j. The interface velocity $F(C(x, y))$ at (x, y) is given by Eq. (16). Let us compare the evolution of (x, y) under the above velocity F, and the evolution that will be produced by the VIIM with the extension velocity given in Eq. (17). First, we note that the second term of Eq. (17),

$$\mu \mathrm{div}\left(g(x, y)\frac{\nabla\phi}{|\nabla\phi|}\right), \tag{18}$$

is a smooth extension of the corresponding term of the interface velocity F. Therefore, according to [21], the ϵ-level sets will enclose the zero-level set

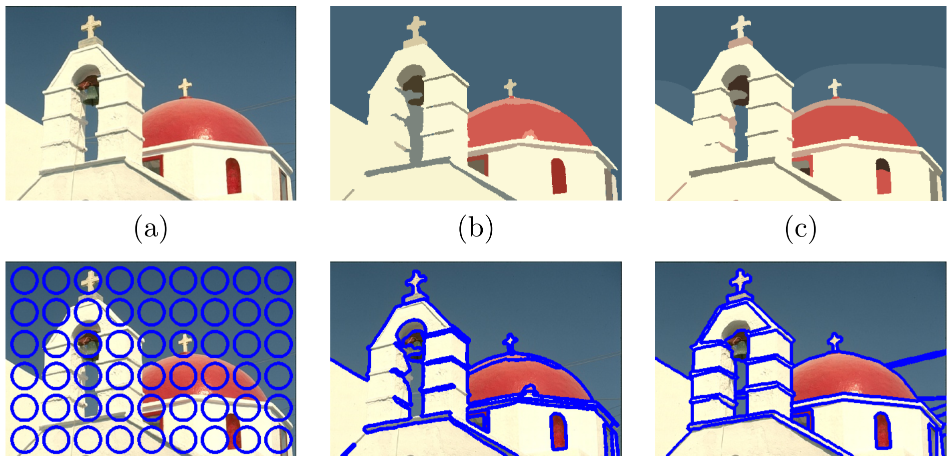

(a) (b) (c)

(d) (e) (f)

Figure 6: Segmentation of an image from the Berkeley Segmentation Dataset. (a) The original image. (b) Regions found by our method, colored according to their mean intensity values. (c) Segmentation obtained using [7], with $K = 8$, $\lambda = 5.0$. (d) Initial contour used by our method. (e) Region boundaries obtained by our method. (f) Groundtruth segmentation from the Berkeley Segmentation Dataset.

in the process of evolution, ensuring that the reconstructed interface will indeed evolve in the correct direction.

Now, let us examine the evolution of a point $(x, y) \in C_{ij}$ under the first term of the extension velocity. For $\epsilon \ll 1$, the contour C and its two ϵ-level sets can be assumed to be locally parallel, and thus their normal directions are collinear. Therefore, we may restrict our analysis to one dimension, in the direction of the contour normal $\mathbf{n}$, such that the contour, or the zero level set of ϕ, is positioned at the origin in this new coordinate system. The illustration of the above is shown in Fig. 7.

Let us assume, w.l.o.g., that $(I-c_i)^2 < (I-c_j)^2$. Therefore, the velocity $F = -\left((I-c_i)^2 - (I-c_j)^2\right)$ is positive, and the point $(x, y) \in C$ is displaced in the positive direction $\mathbf{n}$. According to Eq. (17), the displacements of the two ϵ-level sets are $F_i = -(I-c_i)^2\mathbf{n}$ and $F_j = -(I-c_j)^2\mathbf{n}$. According to the VIIM, the reconstructed contour will lie half-way between the two new ϵ-level sets, that is, the contour will move by $\frac{1}{2}\left(F_i + F_j\right)) > 0$ in the positive direction $\mathbf{n}$, similar to the original contour evolution. A graphical interpretation of the proof is shown in Fig. 7.

Therefore, for $\epsilon \ll 1$, the VIIM with the extension velocity F_{ext} defined

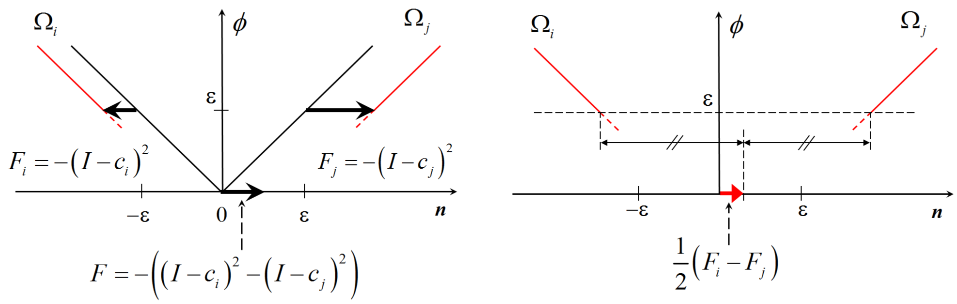

Figure 7: Schematic description of contour evolution under the first term of the extension velocity defined in Eq. (17). (a) The contour is expected to evolve with the velocity F, while its two ϵ-level set evolve with their corresponding extension velocities. The evolution rates are shown with black arrows. (b) The contour evolution, shown with red arrow, obtained using the VIIM method. Its direction coincides with the original direction of F.

in Eq. (17) indeed evolves the zero-level set of the level set function in the same direction as the original interface velocity F defined in Eq. (16). ■

References

[1] D. Adalsteinsson and J.A. Sethian. A fast level set method for propagating interfaces. *Journal of Computational Physics*, 118(2):269–277, 1995.

[2] T. Amiaz and N. Kiryati. Piecewise-smooth dense optical flow via level sets. *International Journal of Computer Vision*, 68(2):111–124, 2006.

[3] T. Brox and D. Cremers. On local region models and a statistical interpretation of the piecewise smooth Mumford-Shah functional. *International journal of computer vision*, 84(2):184–193, 2009.

[4] T. Brox and J. Weickert. Level set segmentation with multiple regions. *Image Processing, IEEE Transactions on*, 15(10):3213–3218, 2006.

[5] V. Caselles, F. Catté, T. Coll, and F. Dibos. A geometric model for active contours in image processing. *Numerische Mathematik*, 66(1):1–31, 1993.

[6] V. Caselles, R. Kimmel, and G. Sapiro. Geodesic active contours. *International journal of computer vision*, 22(1):61–79, 1997.

[7] A. Chambolle and T. Pock. A first-order primal-dual algorithm for convex problems with applications to imaging. *Journal of Mathematical Imaging and Vision*, 40(1):120–145, 2011.

[8] T.F. Chan and L.A. Vese. Active contours without edges. *Image Processing, IEEE Transactions on*, 10(2):266–277, 2001.

[9] D. Cremers, T. Kohlberger, and C. Schnörr. Shape statistics in kernel space for variational image segmentation. *Pattern Recognition*, 36(9):1929–1943, 2003.

[10] D. Freedman and T. Zhang. Active contours for tracking distributions. *Image Processing, IEEE Transactions on*, 13(4):518–526, 2004.

[11] M. Kass, A. Witkin, and D. Terzopoulos. Snakes: Active contour models. *International journal of computer vision*, 1(4):321–331, 1988.

[12] R. Malladi, J.A. Sethian, and B.C. Vemuri. Shape modeling with front propagation: A level set approach. *Pattern Analysis and Machine Intelligence, IEEE Transactions on*, 17(2):158–175, 1995.

[13] O. Michailovich, Y. Rathi, and A. Tannenbaum. Image segmentation using active contours driven by the bhattacharyya gradient flow. *Image Processing, IEEE Transactions on*, 16(11):2787–2801, 2007.

[14] D. Mumford and J. Shah. Optimal approximations by piecewise smooth functions and associated variational problems. *Communications on pure and applied mathematics*, 42(5):577–685, 1989.

[15] S. Osher and J.A. Sethian. Fronts propagating with curvature-dependent speed: algorithms based on hamilton-jacobi formulations. *Journal of computational physics*, 79(1):12–49, 1988.

[16] N. Paragios and R. Deriche. Geodesic active regions: A new framework to deal with frame partition problems in computer vision. *Journal of Visual Communication and Image Representation*, 13(1-2):249–268, 2002.

[17] T. Pock, A. Chambolle, D. Cremers, and H. Bischof. A convex relaxation approach for computing minimal partitions. In *Computer Vision and Pattern Recognition, 2009. CVPR 2009. IEEE Conference on*, pages 810–817. IEEE, 2009.

[18] T. Pock, T. Schoenemann, G. Graber, H. Bischof, and D. Cremers. A convex formulation of continuous multi-label problems. *Computer Vision–ECCV 2008*, pages 792–805, 2008.

[19] C. Sagiv, N.A. Sochen, and Y.Y. Zeevi. Integrated active contours for texture segmentation. *Image Processing, IEEE Transactions on*, 15(6):1633–1646, 2006.

[20] C. Samson, L. Blanc-Féraud, G. Aubert, and J. Zerubia. A level set model for image classification. *International Journal of Computer Vision*, 40(3):187–197, 2000.

[21] R.I. Saye and J.A. Sethian. The Voronoi Implicit Interface Method for computing multiphase physics. *Proceedings of the National Academy of Sciences*, 108(49):19498–19503, 2011.

[22] J.A. Sethian. A fast marching level set method for monotonically advancing fronts. *Proceedings of the National Academy of Sciences*, 93(4):1591, 1996.

[23] A. Tsai, A. Yezzi Jr, and A.S. Willsky. Curve evolution implementation of the Mumford-Shah functional for image segmentation, denoising, interpolation, and magnification. *Image Processing, IEEE Transactions on*, 10(8):1169–1186, 2001.

[24] L.A. Vese and T.F. Chan. A multiphase level set framework for image segmentation using the Mumford and Shah model. *International Journal of Computer Vision*, 50(3):271–293, 2002.

[25] A. Yezzi Jr, A. Tsai, and A. Willsky. A statistical approach to snakes for bimodal and trimodal imagery. In *Computer Vision, 1999. The Proceedings of the Seventh IEEE International Conference on*, volume 2, pages 898–903. IEEE, 1999.

[26] H.K. Zhao, T. Chan, B. Merriman, and S. Osher. A variational level set approach to multiphase motion. *Journal of computational physics*, 127(1):179–195, 1996.

[27] S.C. Zhu and A. Yuille. Region competition: Unifying snakes, region growing, and bayes/mdl for multiband image segmentation. *Pattern Analysis and Machine Intelligence, IEEE Transactions on*, 18(9):884–900, 1996.